MSc in Photonics

PHOTONICS**BCN**

Universitat Politècnica de Catalunya (UPC)
Universitat Autònoma de Barcelona (UAB)
Universitat de Barcelona (UB)
Institut de Ciències Fotòniques (ICFO)

http://www.photonicsbcn.eu

Master in Photonics

MASTER THESIS WORK

STOKES POLARIMETERS BASED ON LIQUID CRYSTALS

Alba Peinado Capdevila

Supervised by Dr. Juan Campos, (UAB)

Presented on date 15th July 2010

Registered at

Escola Tècnica Superior d'Enginyeria de Telecomunicació de Barcelona

Stokes polarimeters based on Liquid Crystals

Alba Peinado Capdevila
Grup d'Òptica, Departament de Física, Universitat Autònoma de Barcelona, Edifici CC, Bellaterra 08193, Spain

E-mail: Alba.Peinado@campus.uab.es

Abstract. In this work, we present a study of different Stokes polarimeters where liquid crystal devices are fundamental elements of the design. These anisotropic materials act as variable retarders controlled electronically. Therefore, it leads to a versatile setup where an optimization of some parameters of the design is essential to minimize the noise propagation. On the one hand, a polarimeter based on two parallel aligned liquid crystal is proposed. Since we can perform any polarization analyzer with this system, we achieve as optimal configuration a set of four analyzers with equispaced distribution in the Poincaré sphere, forming a regular tetrahedron. On the other hand, we analyze a second polarimeter formed by one twisted nematic liquid crystal. Although the optimum configuration is limited by the characteristic curve, we achieve a well-conditioned system with a simpler design. Once the design optimization is done, we carry out an experimental calibration to know exactly the real polarization analyzers used in the laboratory. Finally, we test and compare the two implemented polarimeters and their results are verified with a commercial Stokes polarimeter.

Keywords: Stokes polarimeter, liquid crystal, condition number, optimization.

1. Introduction

A polarimeter is an optical device with the capability of determining the state of polarization (SOP) of a light beam or characterizing a polarizing sample by means of radiometric measurements. Stokes polarimeters measure the SOP of the light beam and characterize the polarization ellipse parameters. Mueller polarimeters determine the matrix which relates the incident and exiting SOPs of a polarizing sample. Polarimetric information becomes essential in many research fields, such as physical medicine [1,2], astronomy [3], material characterization [4], radar applications, among others.

Recently, liquid crystal (LC) displays have been used in polarimetric devices [5-8] by taking the opportunity to modulate the phase dynamically. This feature has an important advantage with respect to a passive polarimeter, as it enables to avoid any mechanical movement and the corresponding uncertainty.

The aim of this work is to simulate, optimize and implement dynamic Stokes polarimeters based on liquid crystal devices. The outline of this work is as follows. First, we give an overview of the mathematics necessary to describe a polarimetric measurement and some indicators useful to the polarimeter optimization. Then, we introduce the design of two different Stokes polarimeters based on LC, the first one uses two parallel aligned LC and the second one is based on one twisted nematic LC. Next, we carry out a numerical optimization of some parameters of the designs to minimize the noise propagation. Afterwards, we simulate different configurations deviated from the optimized one to notice how experimental inaccuracies can affect the system. Next, we develop an experimental calibration of the two polarimetric configurations. Finally, we check the proper working of the instruments by measuring different known SOPs.

2. Mathematical description of polarimetric measurements

In order to describe mathematically the polarimetric properties, different formalisms can be used, such as those developed by Jones [9] or Mueller [10]. In this work, we have used the Mueller-Stokes (M-S) formalism because it allows to deal with unpolarized light. Also, the M-S formalism determines the polarimetric information just by taking intensity measurements. In this framework, the state of polarization of a light beam is expressed with a Stokes vector, which is a column vector of four real components. The first component, S_0, corresponds to the total intensity of the beam, S_1 gives us information about the intensity difference between vertical and horizontal lineal polarizations, S_2 provides the intensity difference between +45º and -45 º lineal polarizations, whereas S_3 corresponds to the intensity difference between right and left circular polarized lights. In addition, the M-S formalism characterizes a polarizing sample with a 4x4 real matrix, so-called Mueller matrix. Then, the interaction of a light beam polarized as the Stokes vector S_{in} with a sample is described as follows,

$$S_{out} = MS_{in} \ , \tag{1}$$

where S_{out} is the Stokes vector of the exiting beam and M is the Mueller matrix of the sample.

A Stokes polarimeter is composed of a polarization-state detector (PSD), which analyses the incoming light beam by measuring the intensity transmitted through a set of polarization analyzers. Each analyzer corresponds to a particular configuration of the polarimeter and is described by a vector analogous to a Stokes vector. If the incident beam has a SOP equal to the analyzer used in the polarimeter, the intensity measured with the PSD is maximum. Mathematically, the PSD is described with *nx4* matrix A. Each matrix row corresponds to a polarization analyzer to which the incident Stokes vector S is projected, and it results the intensity measurement I^k, as the following expression shows.

$$\begin{pmatrix} I^1 \\ I^2 \\ \vdots \\ I^n \end{pmatrix} = \begin{pmatrix} A_0^1 & A_1^1 & A_2^1 & A_3^1 \\ A_0^2 & A_1^2 & A_2^2 & A_3^2 \\ \vdots & \vdots & \vdots & \vdots \\ A_0^n & A_1^n & A_2^n & A_3^n \end{pmatrix} \begin{pmatrix} S_0 \\ S_1 \\ S_2 \\ S_3 \end{pmatrix} \Rightarrow I = AS \tag{2}$$

At least, four independent analyzers are required to determine completely the Stokes vector. While performing more than four intensity measurements leads to a redundant system.

If the matrix A is known thanks to an accurately calibration, we can invert the linear system of equations to isolate the Stokes vector, exactly the information that we want to obtain with the Stokes polarimeter. The simplest case occurs when four linearly independent analyzers are employed, A is of rank four and the inverse matrix of A exists. Therefore, the system has a single solution which is the SOP of the incident beam:

$$S = A^{-1} \cdot I \tag{3}$$

The general case occurs when the polarimeter uses more than four analyzers, A is not a square matrix and there is not a unique solution due to the presence of noise. For searching the solution that minimizes the mean quadratic error, we make use of the pseudo-inverse of the matrix A:

$$S = \left(A^T \cdot A\right)^{-1} \cdot A^T \cdot I = \tilde{A}^{-1} \cdot I \tag{4}$$

It exists an infinite number of analyzers sets, leading to matrices A achieving complete polarimeters. Nevertheless, in presence of noise in the intensity measurements, each matrix A will transmit the error in a different way to the Stokes vector. As a consequence, it is very important to determine the sensitivity of the linear solution to experimental errors in the measurements, in order to optimize the design of the polarimeter. We have used two different quality indicators frequently appearing in the literature: the condition number (CN) [5,8,11] and the equally weighted variance (EWV) [5,12].

The minimization of the condition number indicator quantifies how well-conditioned is the matrix A, i.e. as close as possible to unitary matrix. The definition of this indicator is not unique.

We have used the most usual expression,

$$CN(A) = \frac{\sigma_{\max}}{\sigma_{\min}}, \tag{5}$$

which corresponds to the quotient of the largest over the smallest singular values of matrix *A*. When the matrix *A* is not square, the singular value decomposition theorem is developed, where the matrix is decomposed into a product of three matrices, two orthonormal matrices and a diagonal one in the centre whose elements are the singular values. Unitary matrices have 1 as CN, which do not amplify the error. However, these matrices are not physically possible because Mueller matrices have a limitation in the first column, whose components are the analyzer's intensities.

When the detector system performs more than four measurements, the equally weighted variance becomes more suitable for noticing the improvement due to data redundancy. In fact, this indicator gives us information about the transmission of the variance from the vector *I* to Stokes vector *S*. The expression of this parameter is

$$EWV(A) = \sum_{j=1}^{n} \frac{1}{\sigma_j^2}, \tag{6}$$

where σ_j are singular values of the matrix *A*.

While the EWV expresses the global transmitted variance, we can study separately the variances transmitted at each Stokes coefficient. By analyzing the error propagation of equation (4), we obtain:

$$\delta S_i^2 = \delta I^2 \sum_{k=1}^{N} q_{ik}^2, \tag{7}$$

where q_{ik} are the coefficients of the pseudoinverse matrix *A*, δI is the intensity variance considered constant in all measurements and δS_i is the variance transmitted to the Stokes parameter S_i.

3. Design of polarimeters based on liquid crystals

Liquid crystal (LC) devices are optically anisotropic media which act locally as uniaxial retarders and exhibit optical birefringence. Depending on the external voltage applied, the Mueller matrix describing the element is different. Therefore, by illuminating the LC device we can generate or detect different polarization states controlled electronically. And consequently, these LCs devices are used in dynamic polarimeters. We are going to analyze two different types of nematic LC and the polarimeters that can be implemented by using them. Nematic structure has the molecules aligned in parallel lines although not in layers.

3.1. Parallel aligned nematic liquid crystal

Parallel aligned liquid crystal (PA-LC) has the molecules untwisted between the two walls of the cell, and can be described as a lineal retarder. We represent it mathematically with the Mueller matrix of a waveplate of phase ϕ orientated at θ [10]. Note that its phase is variable and depends on the voltage addressed to the LC element.

A first possibility of polarimetric setup based on PA-LC is sketched in figure 1(a). The PSD is formed by a PA-LC orientated at a fixed angle θ_0 and a polarizer at 0º. The analyzers which can be performed with this specific setup only depend on the LC phase and their expressions are:

$$\vec{A}^k = \left(1, \cos^2 2\theta_0 + \cos\phi \sin^2 2\theta_0, (1-\cos\phi)\sin 2\theta_0 \cos 2\theta_0, \sin\phi \sin 2\theta_0\right)^T \tag{8}$$

Analyzer vectors can be represented in the Poincaré sphere, which gives a visual representation of Stokes vectors. The axes of the sphere are the Stokes components S_1, S_2 and S_3. Consequently, in the sphere equator there are the lineal SOPs while the circular SOPs are mapped at the poles. Any other point in the sphere represents an elliptical SOP. Fully polarized SOPs are on the surface of the sphere of radius 1, while partially polarized SOPs are inside the

sphere. In figure 1(b), we have represented in the same color each set of possible analyzers that can form a PSD, corresponding to a specific angle θ_o of the PA-LC. We observe that PSD analyzers make a circle on the sphere surface, all of them inside a plane. This fact indicates us that we cannot generate a complete basis of the polarization states space with this configuration. This type of polarimeter is called incomplete because it does not allow determining all the Stokes components.

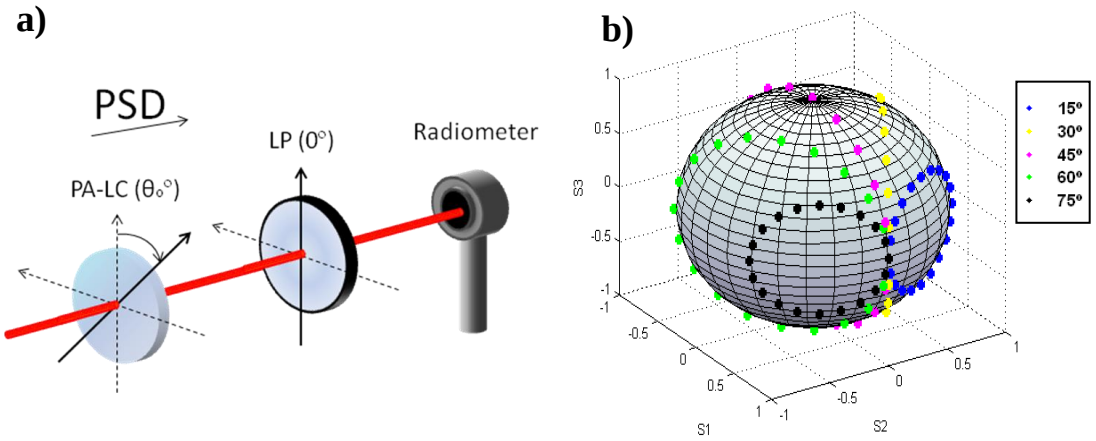

Figure 1. (a) Setup of an incomplete polarimeter based on a parallel aligned liquid crystal followed by a linear polarizer at 0º. (b) Analyzers upon the Poincaré sphere. Each color corresponds to a PSD with a specific angle of the LC. The set of analyzers printed in the same color are obtained by changing the phase of the waveplate from 0º to 360º.

In order to achieve a complete polarimeter, a second PA-LC is added in the setup. The proposed polarimeter, represented in figure 2, is composed of two variable retarders placed at 0º and 45º, followed by a linear polarizer at 0º. The new analyzers,

$$\vec{A}^k = \left(1, \cos\phi_1, \sin\phi_2 \sin\phi_1, \cos\phi_2 \sin\phi_1\right)^T, \tag{9}$$

depend on the two phases of the PA-LCs. In fact, components S_1, S_2 and S_3 are equivalent to the spherical coordinates. As consequence, any point upon the Poincaré sphere representing a polarization analyzer can be generated by sending the right pair of retarders (ϕ_1,ϕ_2). Therefore, this proposed PA-LC configuration allows implementing any set of analyzers obtained in an optimization process without any restriction.

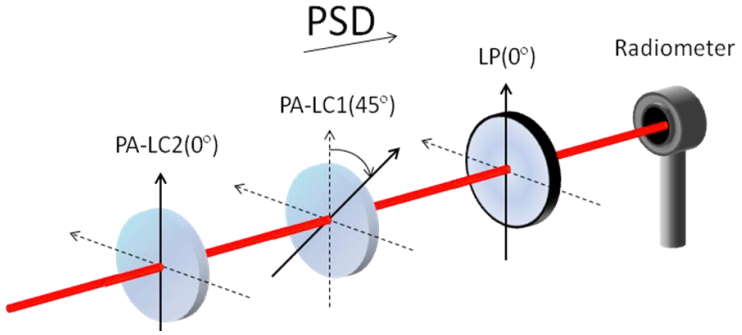

Figure 2. Setup of a complete polarimeter based on two parallel aligned liquid crystals at 0º and 45º, whose retarders are ϕ_2 and ϕ_1 respectively, followed by a linear polarizer at 0º.

3.2. Twisted nematic liquid crystal

Twisted nematic is a type of liquid crystal on which the rubbing directions of the facing cell walls are not parallel, and the direction of the molecules is twisted between the two walls. As a result, the LC cell works as a combination of an elliptical retarder and a rotator [13].

We propose a polarimeter composed of a twisted liquid crystal (TW-LC) placed at 0º acting as a variable waveplate (WP) and a linear polarizer (LP) oriented at a fixed angle, the setup is represented in figure 3(a). To simulate the analyzers which can be obtained with this

polarimeter setup, an experimental calibration of the dynamic waveplate is required. For this purpose, we place the element to characterize in a Mueller polarimeter and the matrices describing the TW-LC for different voltages are obtained. Finally, analyzer vector has the expression:

$$\vec{A}^k = M(V^k)\cdot(1,\cos(2\theta),\sin(2\theta),0)^T, \tag{10}$$

where $M(V^k)$ is the calibrated Mueller matrix of the LC element depending on the addressed voltage and, θ is the polarizer orientation which is kept constant for all the system. We have been working in two methods concerning the Mueller matrices of the WP. First, we have interpolated the experimental data for each coefficient of the matrix; as a result, polynomial functions describing each coefficient at any voltage are obtained. However, due to the inevitable deviations of interpolated functions respect to the real values, the matrices constructed with this method lead to polarization analyzers with non physical sense. For this reason, a second method is implemented where we only use the measured matrices. In fact, the input voltage is approximated to the closest voltage value with an associated calibrated matrix. In figure 3(b) some set of polarization analyzers are mapped on the Poincaré sphere. Each set of analyzers in the same color corresponds to a fixed orientation of the polarizer, so they can be selected to implement a PSD. We emphasize that each PSD curve, printed in the same color, envelops a volume, requirement necessary to have a complete Stokes polarimeter. Therefore, by selecting properly the analyzers we can form a complete basis of the SOP vectorial space. Nevertheless, in the optimization process we have a restriction, the analyzers have to belong to the characteristic curve of the PSD.

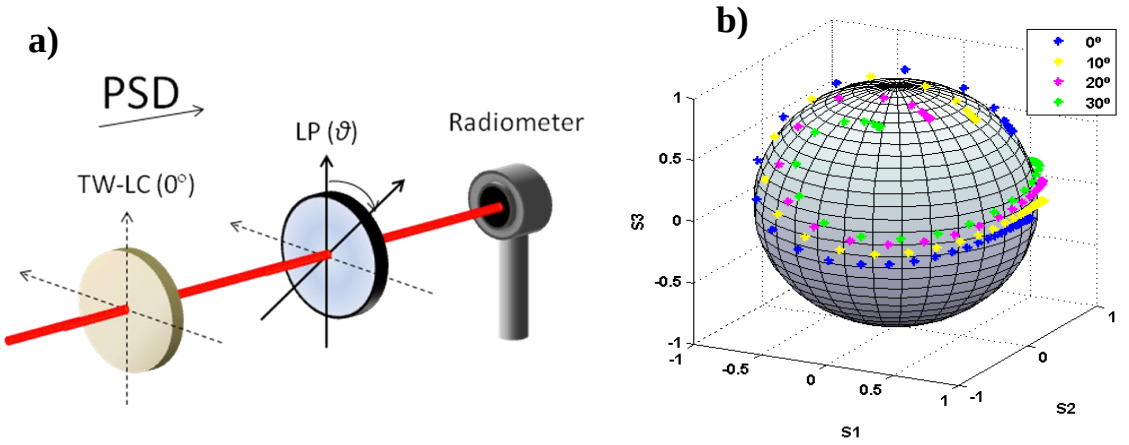

Figure 3. (a) Setup of a complete polarimeter based on one twisted nematic liquid crystal at 0º, followed by a linear polarizer at θº. (b) Set of analyzers upon the Poincaré sphere. Each color corresponds to a PSD with a specific orientation θ of the polarizer, and a ramp of voltages sent to the LC element from 1 to 5 volts.

4. Optimization of the polarimeter design

In this section we are going to optimize two complete polarimetric configurations presented in the last section, the setup based on two PA-LCs and the TW-LC polarimeter. The objective of the optimization process is to select the set of analyzers included in the characteristic curve of the PSD to achieve the minimum noise propagation concerning equation (4).

4.1. Parallel aligned nematic liquid crystal

First, we have carried out a minimization of the indicator CN for the polarimeter based on two PA-LCs. In this configuration, the orientations of their optical elements are fixed as figure 2 indicates, while the LC phases are free variables. Because any analyzer can be performed by properly selecting the pair of phases, the program chooses between any fully polarized state. The computing program begins with 4 polarization analyzers randomly chosen. Then, a MATLAB optimization function minimizes the CN and as a result, a new set of 4 analyzers is

given. To avoid a local minimum, the process is repeated 100.000 times, each step starting with another set of random analyzers. The solution of the program is the set of analyzers with minimum condition number. In figure 4 we represent the four optimal analyzers when there is not any restriction, the minimum CN achieved is 1.732. We observe that analyzers are mapped at the vertices of a regular tetrahedron inscribed in the Poincaré sphere. This result is in agreement with previous studies, as an example in [12]. We have continued the optimization process by studying PSDs composed for more than 4 analyzers in [5]. We have found that when we optimize a set on *n* analyzers, their locations upon the Poincaré sphere coincide with the vertices of a regular polyhedron, when this exists for the specific number *n*. Regular polyhedron gives an analyzer distribution equally separated which maximizes the enclosed volume in the sphere. By maximizing the volume, the corresponding matrix *A* is moving away from a singular matrix and so, leading to the minimum possible CN.

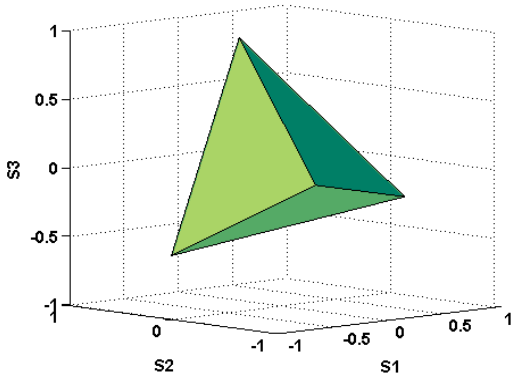

Figure 4. CN minimization for a PSD formed by 4 analyzers. The vertices of the tetrahedron represent the optimal polarization analyzers. The Poincaré sphere is erased to provide an easier visualization.

4.2. Twisted nematic liquid crystal

The parameter optimization of a polarimeter setup based on one TW-LC is carried out in two steps. In the first one, the dependence on the polarizer orientation is analyzed. For this reason, we simulate different PSDs modifying the angle of the polarizer. In all the situations, we address the same sequence of voltages to the dynamic waveplate. Regarding the evolution of the indicator CN in the graph of figure 5, we notice a strong relationship between the indicator and the angle. The minimum CN found by the program appears when the polarizer is placed at 111º. We observe that a small deviation respect to the optimum angle still gives a well-conditioned system.

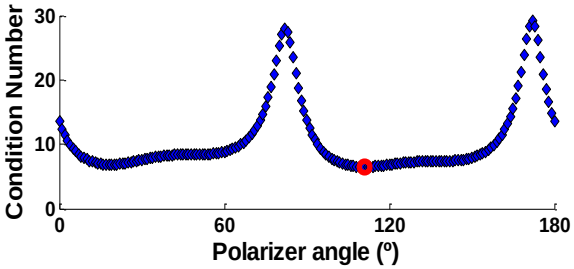

Figure 5. CN as function of the LP orientation for different PSDs by addressing the same sequence of voltages. The red circle marks the minimum CN.

In the second part, the LP is fixed at the optimized angle and we develop a numerical minimization of the EWV figure of merit with respect to four variables (the voltages addressed to the LC when 4 analyzers are used). The program starts with 4 random voltages from 1V to 5V, which is precisely the LC working range. Then, we use a MATLAB function which finds a minimum of a multivariable function. The expression to be minimized, encoded for us, calculates the EWV of a TW-LC polarimetric system when the voltages and the polarizer orientation are given. The result of the minimization function is a new set of 4 voltages corresponding to a PSD with a minimum EWV. In order to avoid a local minimum as solution, the process is repeated 1.000.000 times and in every step, a new set of starting random voltages

is used. The global minimum EWV value and its corresponding set of voltages are the solution of the complete optimization process. In figure 6, we have drawn in blue points the PSD curve, in other words, the set of analyzers that can be chosen by the optimization program. At the same graphic, we have plotted the solution of the EWV minimization (6.89). The distribution of the optimized analyzers can be understood, as well, by considering the importance of equidistance between them and the maximization of the enclosed volume. Because the polyhedron generated with this set of optimal analyzers is an irregular tetrahedron, its CN (4.491) is larger than the CN for the regular tetrahedron. However, this polarimeter is still interesting due to the simplicity of the setup formed by only one liquid crystal device.

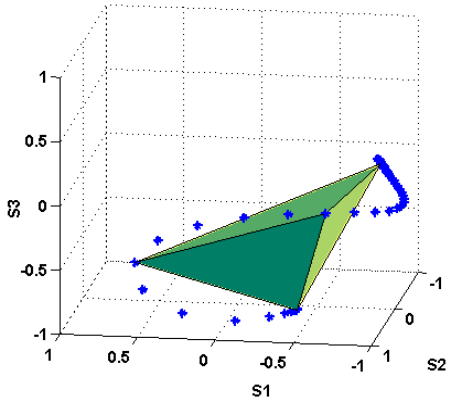

Figure 6. In blue points, possible analyzers on the Poincaré sphere according to the characteristic curve when the polarizer is fixed at 111º. The vertices of the irregular tetrahedron are the set of 4 optimal analyzers, result of minimizing the EWV.

4.3. Simulation of the optimized polarimeters implementation

When we implement the theoretical analyzers to perform the optimized configuration, due to experimental inaccuracies, the polarimeter slightly differs from the theoretical one. We simulate one hundred different polarimeters deviated from the theoretical configuration (i.e. the solution of the numerical optimization), and we study how the quality indicators change. The deviations are implemented by generating zero mean uniformly distributed random values with amplitude 0.2. This study has been done for the PA-LC configuration (see figure 7(a,b)) and for the TW-LC polarimeter (see figure 7(c,d)).

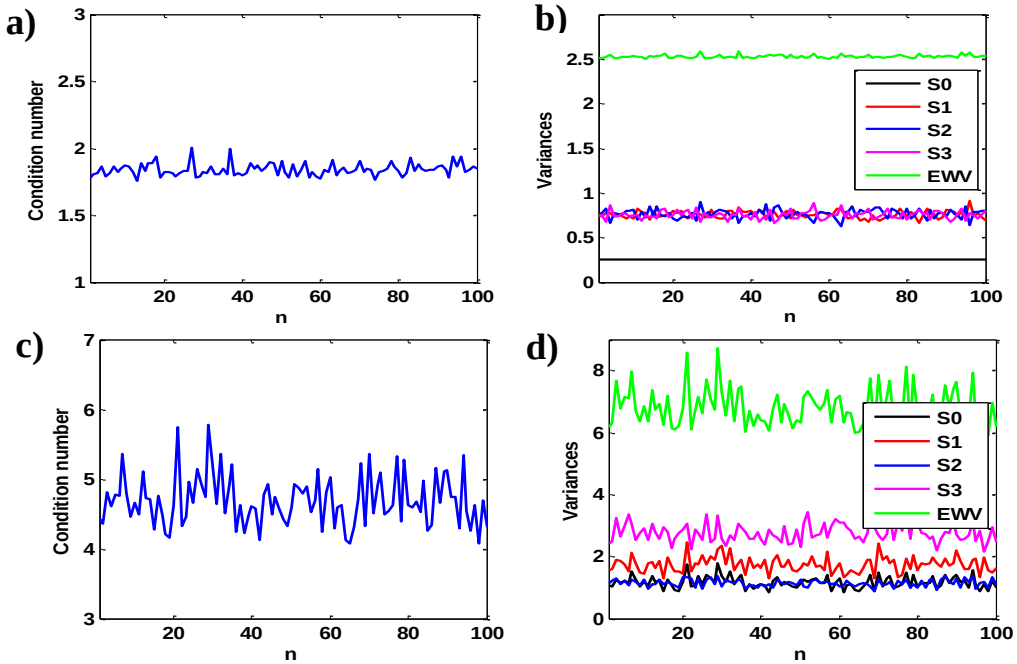

Figure 7. Simulation of 100 polarimeters deviated from the theoretical: (a, b) PA-LC polarimeter and (c, d) TW-LC one. Evolution of (a, c) condition number and (b, d) Stokes variances and EWV.

In both polarimeters we can see that the CN function behaves in essence as the EWV one. Concerning the PA-LC polarimeter, the Stokes variances S_1, S_2 and S_3 are in the same range. On the contrary, Stokes variances related to the TW-LC configuration are different. For instance, S_3 variance is larger than the other two. This difference can be justified by taking into account the location of the analyzers. TW-LC polarimeter has the analyzers closer to the Poincaré sphere equator than the PA-LC configuration, whose analyzers are equidistant distributed. Remember that in the equator S_3 is null, whereas S_1 and S_2 define the lineal SOPs. Finally, we remark that PA-LC polarimeter presents smaller noise propagation and equally distributed variances in the Stokes components, so it is a robust polarimeter, although its setup is more complex than the TW-LC one.

5. Implementation of the optimized polarimeters

5.1. Experimental calibration

The purpose of this section is to calibrate the implementation of the theoretical configuration achieved in the numerical optimization, and therefore to find the real polarization analyzers that are experimentally used at the laboratory.

To perform the PA-LC polarimeter, it is required to know the equivalence between the voltage addressed to each PA-LC (monopixel distributed by Meadowlarks Optics) and the pair of phases obtained in the optimization process, in other words, to determine the look-up table of the liquid crystal device. Once the LC waveplate calibration is done, we can use the phase-voltage function to implement the optimized polarimeter shown in figure 4. Afterwards, we want to calibrate the matrix A to know exactly which configuration we are using. To calibrate the analyzer i, we illuminate the polarimeter in the specific configuration i with four known SOPs (lineal at 0º, 90º and 45º and right circular polarization), and we measure the intensity denoted as I_0, I_{90}, I_{45}, I_{RC}, respectively. Resolving an equation system, we find that the experimental analyzer i has the following expression:

$$A_0^i = \frac{1}{2}\left(I_0^i + I_{90}^i\right); \quad A_1^i = \frac{1}{2}\left(I_0^i - I_{90}^i\right); \quad A_2^i = I_{45}^i - A_0^i; \quad A_3^i = I_{RC}^i - A_0^i; \quad i = 1,...,4 \quad (11)$$

In figure 8(a) we have plotted the calibrated analyzers in red points. We notice that they are slightly different respect to the theoretical ones (green points) due to experimental inaccuracies. However, the calibrated matrix A still gives a well-conditioned system (CN is 2.45).

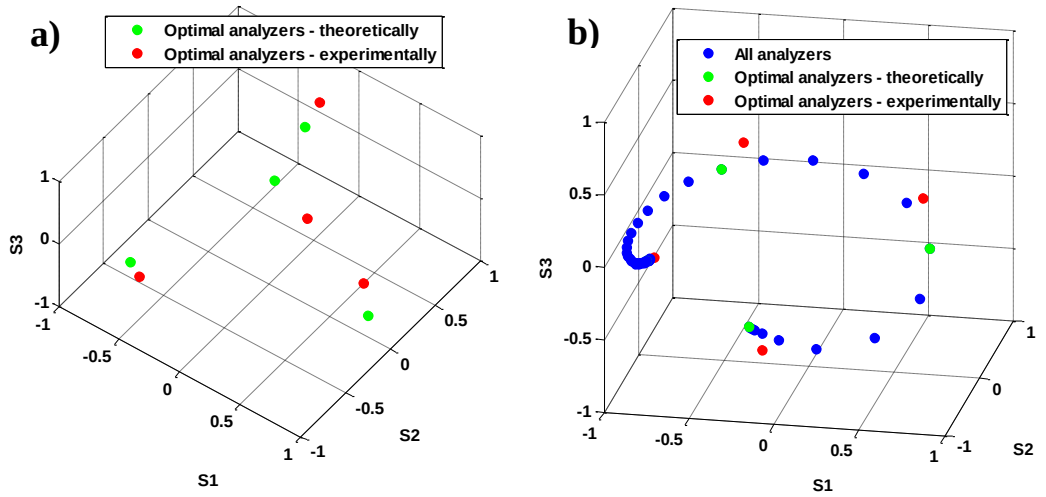

Figure 8. Calibration of the experimental analyzers concerning the polarimeters based on: (a) two parallel aligned LC and (b) one twisted nematic LC.

Next, we calibrate the polarimeter based on one off-the-shelf TW-LC with a mathematical routine known as the Eigenvalue Calibration Method [14]. It requires and calibrates a PSD as well as a PSG (polarization-state generator). Then, it uses different reference samples with a

perfectly known Mueller matrix, although their orientations in the calibration method are not necessary known with accuracy. In fact, their optical characteristics are unambiguously determined during the calibration method. By developing an eigenvalues analysis, the matrix describing the PSD is found. We have used two reference elements, a Glan-Thompson prism polarizer distributed by Casix (PGM5315) and a quarter-wave plate distributed by Thorlabs. Both are placed in 6 different orientations to have robust data. We present in red points the calibrated analyzers in the figure 8(b). Also, the SOPs differ from the theoretical ones, although the associated matrix has a CN (4.61) close to the optimal one. An important reason of the deviation of the experimental analyzers from the characteristic curve is the strongly dependence of liquid crystal retardance on the temperature. Actually, the calibration of the TW-LC Mueller matrices and the calibration of the analyzers have been done in different days. These discrepancies between theory and experimental part emphasize the importance of an experimental calibration done just before using the polarimeter.
We remark that the experimental part of this work has been done by illuminating with a He-Ne laser. Since the LC retarder depends on the illumination wavelength, the calibrated matrices are only valid in the wavelength range around 633nm.

5.2. Testing the polarimeters
To finalize this work, we have tested the two LC polarimeters by measuring three different SOPs. Results are verified with the information given by a commercial polarimeter (Analyzer System, PAN 5710VIS, S/N: M60217605, distributed by Thorlabs). Since the two LC polarimeters tests have been done in different days, we perform two independent sets of measurements. Each of them has its own verification with the commercial polarimeter. Results shown in table 1, are expressed as function of two parameters defining the polarization ellipse: the azimuth and the ellipticity. The specific range of values of the azimuth angle is from 90º to -90º and the corresponding to the ellipticity is from 45º to -45º. In addition, the results are the average of 100 measurements of the same incident SOP. Thus, the standard deviation corresponding to a population of 100 samples is also provided. In the circular SOP measurements, azimuth values are not taken into account because there is not any privileged orientation.
We see an agreement between LC polarimeters results and those given by the commercial polarimeter. Also, we notice that the standard deviation of LC polarimeters is smaller than the error of the commercial polarimeter, therefore the implemented LC polarimeters have a good repeatability.

Table 1. Stokes vectors measured by the two implemented polarimeters and a commercial one.

	Lineal SOP		Right circular SOP		Elliptical SOP	
	Azimuth	Ellipticity	Azimuth	Ellipticity	Azimuth	Ellipticity
PA-LC polarimeter	29.957±0.004	-0.602±0.004	-	43.719±0.066	23.356±0.004	24.146±0.005
Commercial polarimeter	29.961±0.010	-0.491±0.008	-	44.545±0.022	22.384±0.024	23.855±0.009
TW-LC polarimeter	30.356±0.002	-0.598±0.001	-	35.981±0.004	10.719±0.001	-19.133±0.001
Commercial polarimeter	30.234±0.008	-0.412±0.013	-	43.505±0.028	9.963±0.012	-17.670±0.005

6. Conclusions
We have presented a comprehensive study of two complete Stokes polarimeters based on liquid crystal technology. The first one is composed of two parallel aligned LCs and a polarizer, and the second one is formed by one twisted nematic LC and a polarizer. We carried out a numerical optimization in order to minimize the intensity noise propagation. As a result, we found the optimal parameters for the two proposed configurations. Then, we examined different polarimeters deviated from the optimal one, simulating implemented polarimeters with experimental inaccuracies, and we observed that they are still well optimized configurations. In

the PA-LC polarimeter the analyzers are located in the vertices of a regular tetrahedron inscribed in the Poincaré sphere. For this reason, Stokes variances are very similar. However, TW-LC polarimeter has a characteristic curve, and the representation in the Poincaré sphere constituted an irregular tetrahedron where analyzers are closer to the equator. As consequence, Stokes variances concerning lineal contribution are smaller than Stokes variance related to the elliptical contribution. Afterwards, we calibrated both detector systems, with the purpose of determining which are the real analyzers used in the laboratory. Finally, the two LC polarimeters have been tested by measuring diverse incident SOPs and the results are compared with the obtained with a commercial polarimeter. The experimental results obtained are an important indicator of the validity of the optimization methodology provided in this work.
In conclusion, both LC polarimeters are optimized instruments to measure polarization of the light although we appreciate some differences. PA-LC polarimeter allows implementing the regular tetrahedron, the optimal configuration independent of the SOP to be measured. Whereas the TW-LC configuration is an irregular tetrahedron, so the quality indicators are slightly worse although the setup is simpler. In addition, we remark that simple design leads to small experimental errors and a perfect prototype to implement as an instrument with industrial applications.

Acknowledgments
I am indebted to my advisor, Prof. Juan Campos for his help and encouragement throughout the course of this work. I acknowledge financial support from Spanish Ministerio de Ciencia e Innovación (FIS2009-13955-C02-01).

References

[1] K. M. Twietmeyer, R. A. Chipman, Ann E. Elsner, Y. Zhao, and D. VanNasdale, "Mueller matrix retinal imager with optimized polarization conditions," Opt. Express **16**, 21339-21354 (2008).
[2] J. C. Ramella-Roman, D. Duncan, and T. A. Germer, "Out-of-plane polarimetric imaging of skin: Surface and subsurface effects," Proc. SPIE **5686**, 142-153 (2005).
[3] N. Uribe-Patarroyo, A. Álvarez-Herrero, R. L. Heredero, J. C. del Toro Iniesta, A. C. López Jiménez, V. Domingo, J. L. Gasent, L. Jochum, V. Martínez Pillet, and The IMaX Team, "IMaX: a polarimeter based on liquid crystal variable retarders for an aerospace mission," Phys. Status Solidi C 5, 1041-1045 (2008).
[4] A. Márquez, I. Moreno, C. Iemmi, A. Lizana, J. Campos, and M.J. Yzuel, "Mueller-Stokes characterization and optimization of a liquid crystal on silicon display showing depolarization," Opt. Express **16**, 1669-1685 (2008).
[5] A. Peinado, A. Lizana, J. Vidal, C. Iemmi, and J. Campos, "Optimization and performance criteria of a Stokes polarimeter based on two variable retarders," Opt. Express, **18**, 9815-9830 (2010).
[6] E. Garcia-Caurel, A. De Martino, and B. Drévillon, "Spectroscopic Mueller polarimeter based on liquid crystal devices," Thin Solids Films **455-456**, 120-123 (2004).
[7] J. M. Bueno, "Polarimetry using liquid-crystal variable retarders: theory and calibration," J. Opt. A: Pure Appl.Opt. **2**, 216-222 (2000).
[8] A. De Martino, Y. K. Kim, E. Garcia-Caurel, B. Laude, and B. Drévillon, "Optimized Mueller polarimeter with liquid crystal," Opt. Letters **28**, 616-618 (2003).
[9] R. C. Jones, "A new calculus for the treatment of optical systems," J. Opt. Soc. Am. A **31**, 488-493 (1941).
[10] D. Goldstein, *Polarized Light*, (Marcel Dekker, NY, 2003).
[11] P.Taylor, *Theory and Applications of Numerical Analysis*, (Academic Press, London, 1974).
[12] D.S. Sabatke, M.R. Descour, E.L. Dereniak, W.C. Sweatt, S.A. Kemme, and G.S. Phipps, "Optimization of retardance for a complete Stokes polarimeter," Opt. Letters **25**, 802-804 (2000).
[13] A. Márquez, J. Campos, M. J. Yzuel, I. Moreno, J. A. Davis, C. Lemmi, A. Moreno, and A. Robert, "Characterization of edge effects in twisted-nematic liquid-crystal displays," Opt. Eng. **39** 3301–7 (2000).
[14] E. Compain, S. Poirier, and B. Drevillon, "General and Self-Consistent Method for the Calibration of Polarization Modulators, Polarimeters, and Mueller-Matrix Ellipsometers," Appl. Opt. **38**, 3490-3502 (1999).